ACADEMIC PRESS

Available online at www.sciencedirect.com
SCIENCE DIRECT®

Journal of Catalysis 214 (2003) 273–283

JOURNAL OF CATALYSIS

www.elsevier.com/locate/jcat

Dehalogenation of 1-chloro-1-fluoroethene to acetylene on α-Cr_2O_3 $(10\bar{1}2)$

Steven C. York and David F. Cox *

Department of Chemical Engineering, Virginia Polytechnic Institute and State University, Blacksburg, VA 24061, USA

Received 7 August 2002; revised 27 September 2002; accepted 8 October 2002

Abstract

The adsorption of $CFCl{=}CH_2$ on the nearly stoichiometric Cr_2O_3 $(10\bar{1}2)$ surface results in a 1,1-dihaloelimination reaction to produce acetylene gas, $HC{\equiv}CH_{(g)}$, and adsorbed chlorine and fluorine. Thermal desorption experiments reveal two acetylene desorption features. The lower temperature acetylene channel is desorption limited ($E_a = 92$ kJ/mole), while the formation of fluorovinyl and/or vinylidene surface intermediates is suggested by the occurrence of a higher temperature ($E_a = 124$ kJ/mole) reaction-limited acetylene desorption channel. The deposition of halogen onto the sample surface by the $CFCl{=}CH_2$ decomposition reaction was found to initially increase the $CFCl{=}CH_2$ sticking coefficient and the activity for halogen coverages up to about one-third and then lead to deactivation at higher halogen coverages due to site blocking of the surface cations. No evidence was seen for the replacement of surface lattice oxygen by halogen under the conditions of this study. Surfaces that were preexposed to O_2 to site block surface cations with terminal chromyl oxygen were found not to react with $CFCl{=}CH_2$.
© 2003 Elsevier Science (USA). All rights reserved.

Keywords: Cr_2O_3; Single crystal; Chromia; 1-chloro-1-fluoroethene; Dehalogenation; Vinyl; Vinylidene; α-elimination

1. Introduction

Much of the literature concerning halocarbon chemistry over Cr_2O_3 has been devoted to compounds that are intermediates or byproducts formed during the manufacture of alternative refrigerant compounds [1–4]. Unsaturated halocarbons are used as feedstocks for the manufacture of industrially important hydrochlorofluorocarbons (HCFCs) and are often cited as both intermediates and nonselective reaction products [1,4].

Vecchio et al. [5] studied the fluorination (replacement of chlorine or hydrogen by fluorine) of a number of halocarbons over aluminum fluoride (AlF_3) catalysts and observed many of the same reactions that were later reported over Cr_2O_3 and other fluorination catalysts [1,4,6]. They observed that fluorination is the dominant reaction in the presence of HF, but that HF and HCl abstraction from haloethanes occurs in the absence of HF. A build-up of HX (X = Cl or F) on the surface was found to cause the subsequent readdition of HF and HCl to haloethenes. The readdition of HX, combined with the exchange of halogen between the HCFC molecules and the surface, results in a broad mix of saturated and unsaturated products.

The chemistry observed over Cr_2O_3 powders is similar to that found over AlF_3 [7]. Kavanagh et al. used deuterated hydrofluoric acid, DF, to study both the addition of HF to trichloroethene (TCE) and the subsequent halogen exchange reactions over a powdered Cr_2O_3 microcrystalline catalyst pretreated with HF [8]. They reported that HX addition/elimination reactions and direct halogen exchange with the surface may both occur for HCFCs over Cr_2O_3. In deuterium labeling experiments using DF and TCE, the label indicated that HX addition to TCE follows the Markovnikov rule. The incorporation of only a single deuterium label in product molecules containing multiple fluorine atoms indicated that haloalkanes must undergo F-for-Cl exchange with a halogen species on the catalyst surface. Multiple HF elimination/DF addition steps would have resulted in more deuterium labels in the product. The addition of HF across the C=C double bond was postulated to occur as a first step in the reaction of HF and TCE. Subsequent fluorination is though to occur via direct halogen exchange with the surface. Hydrofluorination of TCE at 523 K was reported to yield about 90% CF_3CH_2Cl (HCFC-133a). The cation oxi-

* Corresponding author.
E-mail address: dfcox@vt.edu (D.F. Cox).

0021-9517/03/$ – see front matter © 2003 Elsevier Science (USA). All rights reserved.
doi:10.1016/S0021-9517(02)00033-7

dation state was reported as Cr^{3+}, but no specific information concerning the catalyst surface was offered.

Kemnitz and co-workers [6,9] used deuterium labeled HCl (DCl) to study CHF_2CHF_2 isomerization to CF_3CH_2F (HFC-134 $\leftrightarrows$ HFC-134a). For microcrystalline Cr_2O_3 pretreated with HF, isomerization proceeds via HF elimination to form $CF_2{=}CHF$ followed by readdition of HF, in accordance with the Markovnikov rule, to form CF_3CH_2F. Interestingly, if the catalyst was pretreated using DCl then a complex set of reactions ensued that included HX elimination, and both Markovnikov and anti-Markovnikov HX addition. The presence of Cl on the Cr_2O_3 surface was found to promote the formation of a broad range of saturated and unsaturated products. This result echoes the earlier work of Vecchio and co-workers [5], who made similar observations for AlF_3.

Brunet et al. [4] have studied the reaction of CF_3CH_2Cl (HCFC-133a) over Cr_2O_3 powder and report HF elimination both in the presence and in the absence of HF. Over Cr_2O_3 samples that were not prefluorinated and in the absence of added HF, formation of $CF_2{=}CHCl$ (HCFC-1122a) was reported as the primary reaction product. The overall reaction was reported as

$$CF_3CH_2Cl \leftrightarrows CF_2{=}CHCl + HF.$$

At equilibrium, approximately equal amounts of HCFC-1122a and HCFC-133a were found in the reaction mix. Brunet et al. report that no surface chlorine was observed with XPS on the catalyst following HCFC-133a reaction in the absence of HF. Direct exposure of the surface to HF at 280 °C for 2 h was found to result in an XPS F/Cr ratio of 0.36.

Freund and co-workers [10,11] have studied the adsorption of ethene in ultrahigh vacuum (UHV) over stoichiometric and oxygen-exposed Cr_2O_3 (0001) films that were epitaxially grown on Cr (110). Over the stoichiometric surface they report that ethene forms a π-complex at surface cation sites that has a desorption temperature of 220 K. This temperature corresponds to a first order activation energy for desorption of around 57 kJ/mol using the Redhead method [12]. Surfaces that were preexposed to oxygen were found to adsorb ethene only at defect sites, strongly attenuating the ethane uptake for an oxygen-saturated surface. Scarano et al. [13] reported similar findings over Cr_2O_3 microcrystals that contained predominantly $(10\bar{1}2)$ faces. Both groups [10,11,13] have suggested that the ethene molecule is arranged with its molecular axis parallel to the Cr_2O_3 surface. Both groups also suggest that surface/adsorbate bond formation results in a small amount of charge transfer from the molecule to the surface with minimal backbonding by the Cr^{3+} cations. The lack of backbonding by cations on the nearly stoichiometric Cr_2O_3 $(10\bar{1}2)$ surface (the object of the present investigation) is also suggested by the low, (195 K), desorption temperature of CO. The low activation energy for desorption (50 kJ/mol [12]) for the well-known electron acceptor CO, indicates that the surface–adsorbate interaction is predominantly sigma and that backbonding is minimal on the nearly stoichiometric surface (S.C. York, D.F. Cox, unpublished results).

While a number of surface science studies of haloalkene adsorption and reaction have been reported for metal surfaces, this work is the first reported study of the reaction of an unsaturated halocarbon over single crystal Cr_2O_3.

2. α-Cr_2O_3 surfaces studied

The Cr_2O_3 $(10\bar{1}2)$ surface has been characterized in previous work [14]. The ideal stoichiometric surface has only one local coordination environment for the surface cations and anions. A ball model representation of the ideal, stoichiometric surface is shown in Fig. 1. The topmost atomic layer of the ideal surface is composed entirely of oxygen anions. The surface is nonpolar, and one full stoichiometric repeating unit normal to the surface contains five atomic layers arranged as [O, Cr, O, Cr, O]. The surface has a rectangular (almost square) periodicity with a ratio of sides of $a/b = 0.94$. At the ideal $(10\bar{1}2)$ surface, all O^{2-} anions in the top atomic layer are three-coordinate with a pyramidal local coordination, and the Cr^{3+} cations in the second atomic layer are five-coordinate. Both ions have one degree of coordinate unsaturation relative to their bulk counterparts [15]. All ions below the top two atomic layers are fully coordinated. A nearly stoichiometric surface can be

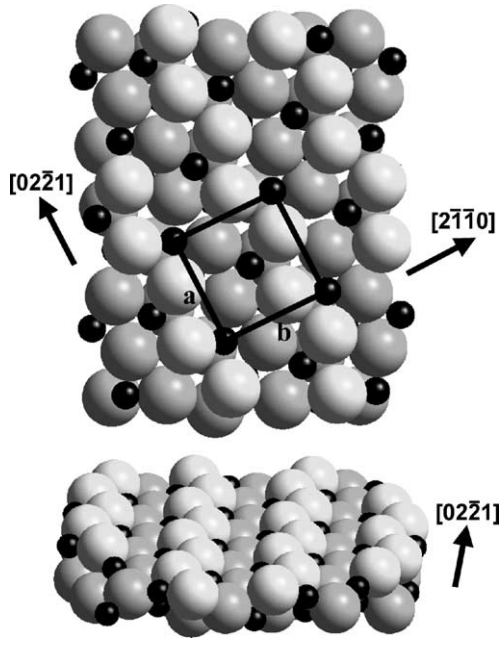

Fig. 1. Ball model illustration of the ideal, stoichiometric Cr_2O_3 $(10\bar{1}2)$ surface. The top view shows the $(10\bar{1}2)$ surface parallel to the plane of the page. A surface unit cell is drawn to show the periodicity. The bottom illustration shows a side view of one stoichiometric repeating layer. The chromium cations are represented by small black spheres and oxygen anions by the large gray spheres.

prepared by Ar^+ ion bombardment and annealing in vacuum at 900 K [14].

In addition to the nearly stoichiometric surface, the surface can be prepared with the cations capped with terminal chromyl oxygen (Cr=O). This oxygen-terminated surface is prepared by repeated low-temperature O_2 exposures on a nearly stoichiometric surface until nearly all surface cations are capped with terminal oxygen [14]. The oxygen-terminated surface exposes both three-coordinate O^{2-} anions and terminal chromyl oxygen (Cr=O) [14].

3. Experimental methods

The reaction of $CFCl{=}CH_2$ (HCFC-1131a) over stoichiometric and oxygen-terminated (1×1) Cr_2O_3 $(10\bar{1}2)$ surfaces was investigated using thermal desorption spectroscopy (TDS), Auger electron spectroscopy (AES), and low-energy electron diffraction (LEED). Experiments were conducted in an ion-pumped UHV chamber, equipped with a Physical Electronics Model 15-155 single-pass CMA for AES, an Inficon Quadrex 200 mass spectrometer for TDS and a set of Vacuum Generators 3-grid reverse view LEED optics. The base operating pressure for this study was 1×10^{-10} Torr. AES data were collected using an incident electron beam of 5 keV for all measurements. Spectra were collected in N(E) mode and differentiated numerically. Electron stimulated reduction of the surface was not observed to occur during AES experiments. A broad-beam ion gun was used for sample cleaning (sputtering).

The crystal was oriented to within 1° of the $(10\bar{1}2)$ surface using Laue backreflection and polished to a final mirror finish with 0.25-μm diamond paste. The sample was mechanically clamped onto a tantalum stage that was fastened to LN_2-cooled copper electrical conductors. A Type K thermocouple was attached through a hole in the stage to the back of the single crystal using Aremco #569 ceramic cement. This arrangement allowed direct measurement of the sample temperature.

PCR Inc. 1-chloro-1-fluoroethene ($CFCl{=}CH_2$) (97%), Matheson acetylene (HC≡CH) (99.6%), Matheson oxygen (99.997%), and Matheson deuterium (99.997%) were used as received. The 1-chloro-1-fluoroethene was analyzed by mass spectrometry for acetylene ($m/z = 26$) contamination and none was found. Gas dosing was accomplished by backfilling the chamber through a variable leak valve. All doses for $CFCl{=}CH_2$ and acetylene TDS experiments were conducted at 163 K. All dose sizes have been corrected for ion gauge sensitivity, and desorption quantities have been corrected for mass spectrometer sensitivity [16–18].

A nearly stoichiometric, (1×1) surface was prepared by ion-bombardment followed by annealing to 900 K. The oxygen-terminated surface was prepared by repeated 0.2-L oxygen exposures at 163 K, following preparation of the stoichiometric (1×1) surface. Oxygen saturation of the surface was confirmed using TDS and AES, which both indicate a concentration of adsorbed oxygen corresponding to nearly one oxygen atom per surface Cr^{3+} cation [14]. The oxygen-saturated surface consists almost entirely of fully coordinated chromium cations, capped by terminal oxide ions, Cr=O.

AES measurements were conducted at 800 K to avoid sample charging. Because of overlap between the primary oxygen and chromium Auger peaks, the surface chromium concentration was followed by measuring the Cr $L_{2,3}M_{2,3}M_{2,3}$ (490 eV) peak-to-peak height [14]. Atomic Cl/Cr ratios were estimated with AES using appropriate sensitivity factors for the Cl KLL signal [19] and the Cr $L_{2,3}M_{2,3}M_{2,3}$ signal [14].

4. Results

$CFCl{=}CH_2$ was found to react readily with the ordered, nearly stoichiometric Cr_2O_3 $(10\bar{1}2)$ surface. Following a product search that included all mass numbers (m/z) from 2 to 200, acetylene (HC≡CH) was determined to be the single gas-phase product formed. Specifically, no fluoroacetylene, chloroacetylene, HCl, or HF gas-phase reaction products were observed during TDS. The HC≡CH (g) product identification was made by comparison of a measured mass spectrometer cracking pattern for an acetylene standard with thermal desorption peak intensities. The relative intensities of four m/z signals (27, 26, 25, 13) were used to positively identify acetylene. The measured acetylene cracking pattern is in good agreement with published data for acetylene [20]. The primary mass peak for acetylene was found to be $m/z = 26$, and this mass number was monitored when recording acetylene desorption signals. AES was used to demonstrate that halogen removed from the reactant molecule remains on the sample surface following reaction.

4.1. $CFCl{=}CH_2$ thermal desorption from a nearly stoichiometric surface

The top and bottom panels in Fig. 2 show desorption traces of reactant and product from $CFCl{=}CH_2$ TDS experiments initiated on a nearly stoichiometric (1×1) Cr_2O_3 $(10\bar{1}2)$ surface. Consecutive doses of 0.06 and 0.03 L were selected to show the product and reactant, respectively. Both reactant and product desorption features undergo peak temperature shifts and significant intensity changes. The dose sizes in the desorption traces shown were chosen in order to best illustrate the changes observed for each peak.

4.1.1. $CFCl{=}CH_2$ desorption

The top panel of Fig. 2 follows desorption of the dosed molecule, $CFCl{=}CH_2$ ($m/z = 80$), during a TDS series of consecutive 0.03 L doses initiated over a nearly stoichiometric (1×1) Cr_2O_3 $(10\bar{1}2)$ surface. The peak desorption temperature is 180 K following the first dose and shifts upwards to 200 K by 0.10 L of total exposure.

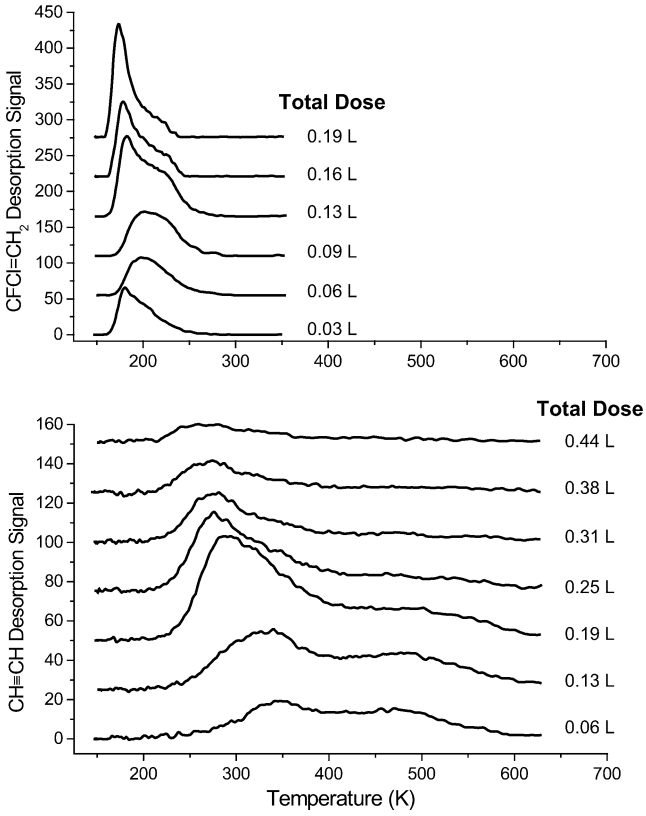

Fig. 2. $CFCl{=}CH_2$ thermal desorption traces for consecutive runs with fixed dose sizes beginning with a clean, stoichiometric surface. The top panel shows the variation in desorption behavior of the $CFCl{=}CH_2$ reactant for consecutive 0.03 L doses. The bottom panel shows the variation in desorption behavior of the product HC≡CH product for consecutive 0.06 L doses. The relative intensities have been corrected for mass spectrometer sensitivity.

In subsequent doses the intensity of the 200-K feature increases and the 180-K feature reappears. As the total dose reaches 0.16 L, the intensity of the 200-K feature decreases, leaving the 180-K feature as the primary contribution in the desorption spectrum. The initial upward shift in peak desorption temperature of around 20 suggests that the surface–adsorbate interaction is initially strengthened by $CFCl{=}CH_2$ exposure (initial surface halogenation), but this effect is reversed for total exposures beyond about 0.16 L.

In TDS experiments conducted using larger dose sizes the upward shift in peak desorption temperature is missed because the majority of $CFCl{=}CH_2$ detected arises from the 180-K feature. For dose sizes of 0.13 L or more, the feature at 200 K only appears as a small, high-temperature shoulder.

4.1.2. Product HC≡CH desorption

For a series of consecutive 0.06 L doses, the acetylene product desorption occurs in two temperature regions, as seen in the bottom panel of Fig. 2. Peak desorption temperatures of 350 and 470 K are observed for acetylene on the initial TDS run (0.06 L). In the second and third TDS runs, the low-temperature (350-K) peak grows in intensity and shifts down in temperature to 280 K. The high-temperature (470-K) feature remains relatively unchanged for total exposures below 0.19 L.

Following 0.19 L of total $CFCl{=}CH_2$ exposure, the low-temperature acetylene peak continues to shift to lower temperatures, but gradually decreases in intensity with each successive TDS run. The high-temperature acetylene peak rapidly loses intensity for total exposures of 0.25 L and greater. The 470 K desorption temperature for the high-temperature HC≡CH feature does not appear to change significantly as desorption intensity declines. AES experiments following various $CFCl{=}CH_2$ exposures demonstrate that the initial increase in activity and the eventual deactivation of the surface are linked to the degree of halogenation of surface cation sites (see below).

In addition to the results shown in Fig. 2, TDS experiments (not shown) with $CFCl{=}CH_2$ were also performed following the preadsorption of D_2 in an attempt to combine the active surface intermediate with surface D. In the event of the reaction of the surface intermediate with preadsorbed D atoms, the possibility exists of determining the number of intermediate/surface bonds by the number of incorporated D atoms. Specifically, the presence of DC≡CH as a desorption product could demonstrate that the reaction mechanism proceeds through an acetylide (–C≡CH) intermediate, recombining with surface hydrogen prior to desorption. No DC≡CH was detected in either the low-temperature or high-temperature states, suggesting that a recombination step is not involved. However, the results are not completely conclusive because D_2 was found to desorb at 285 K, well below the 470-K feature for acetylene desorption.

4.1.3. Chemisorbed acetylene

TDS was also used to investigate the desorption kinetics of chemisorbed acetylene. Fig. 3 shows acetylene desorption

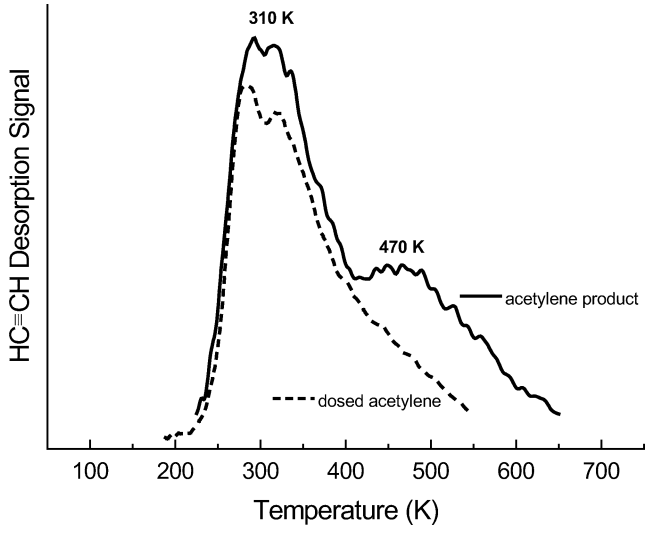

Fig. 3. Comparison of the desorption behavior for dosed, chemisorbed acetylene (dashed line), and product acetylene from the reaction of $CFCl{=}CH_2$ (solid line). The traces demonstrate that the low-temperature acetylene feature is desorption limited, while the high temperature feature is reaction limited.

following a 0.03 L dose of HC≡CH at 163 K on a nearly stoichiometric surface. Also shown for comparison is a TDS trace for product acetylene formed from a 0.06 L dose of $CFCl{=}CH_2$. Small doses of acetylene yield a single desorption feature near 325 K. No reaction of acetylene with the surface is observed. Specifically, water, CO, and CO_2 were not observed as desorption products and AES shows no surface carbon following acetylene TDS experiments.

The desorption temperature of dosed acetylene coincides with the lower temperature (350–270 K) feature from the acetylene product. Similarities between the desorption temperatures and peak shapes of the acetylene product and dosed acetylene indicate that the low-temperature HC≡CH feature is desorption limited. The 470-K feature is not observed following acetylene adsorption at 163 K, demonstrating that the higher temperature product feature is reaction-limited.

4.2. Post-reaction AES analysis

Fig. 4 shows the increase in the surface AES Cl/Cr ratio observed for a TDS series of consecutive 0.13-L doses of $CFCl{=}CH_2$ begun over a clean, nearly stoichiometric surface. The F/Cr is not shown because fluorine was found to undergo rapid electron stimulated loss from the surface and could not be quantified. (Note that small F AES signals have been observed in very short (1–2 s) scans of a narrow range of kinetic energy immediately upon sample introduction into the electron beam, but the F is removed before a sufficient signal-to-noise can be reached for quantitative analysis.) The Cl/Cr ratio is observed to increase linearly following each $CFCl{=}CH_2$ dose until a total exposure of around 0.5 L. Between 0.5 and 1.0 L of total exposure, the Cl/Cr ratio levels off at a maximum value of around 0.16. The surface O/Cr ratio was measured before (nearly stoichiometric surface) and after $CFCl{=}CH_2$ TDS experiments and found not to change due to the deposition of surface halogen. Hence, no evidence was seen for the replacement of lattice oxygen by halogen under these thermal desorption conditions. Additionally, no evidence was seen for the deposition of surface carbon.

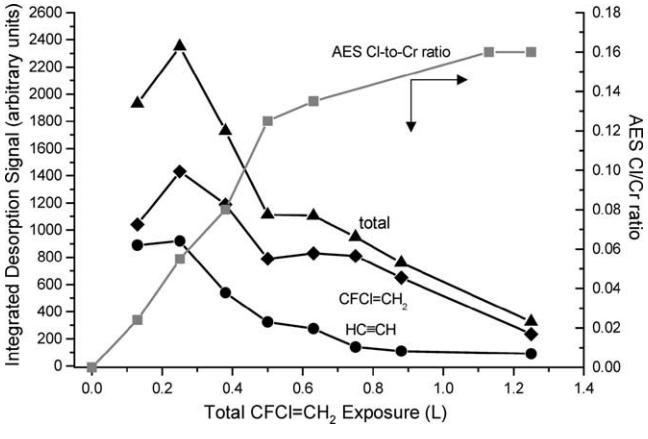

Fig. 4. Comparison of thermal desorption yields for consecutive doses to the resulting surface Cl/Cr ratio determined by AES. The AES Cl/Cr ratio is read from the right hand axis, while the integrated desorption intensities are read from the left hand axis. The integrated desorption intensities have been corrected for mass spectrometer sensitivity. See text for discussion.

Fig. 4 also shows the relative quantities (integrated desorption signals) of $CFCl{=}CH_2$ and HC≡CH desorbed from the surface during a TDS series of consecutive 0.13-L doses of $CFCl{=}CH_2$. The amounts of both reactant and product desorbed from the surface are observed to increase initially and then to steadily decrease. Acetylene production and chlorine deposition are observed to cease around 1.0 L of total exposure. Surfaces that have a Cl/Cr ratio of 0.16 following $CFCl{=}CH_2$ TDS experiments no longer produce acetylene product and are described as "deactivated."

The total (sum) of both desorbing species is also shown in Fig. 4. Changes in the total are indicative of changes in the sticking coefficient of $CFCl{=}CH_2$. Initially, the total increases, but, beyond around 0.25 L of total exposure, the total amount of desorbing species declines, indicating a decrease in the $CFCl{=}CH_2$ sticking coefficient as the chemistry shuts down. The maximum value of the sticking coefficient occurs at a surface Cl/Cr ratio of 0.055.

Consecutive TDS runs using various $CFCl{=}CH_2$ dose sizes (0.03–1.0 L) were carried out until acetylene production ceased and all were found to yield a final AES Cl/Cr ratio of 0.16, regardless of the dose size and total exposure. As demonstrated elsewhere (S.C. York, D.F. Cox, J. Phys. Chem. B, in press), a Cl/Cr ratio (or X/Cr ratio) of 0.32 represents essentially one adsorbed chlorine (halogen) atom per surface cation. A Cl/Cr ratio of 0.16 implies that approximately half of the surface cations are capped by adsorbed chlorine. Fig. 5 shows an AES spectrum of a halogenated sample surface having a Cl/Cr ratio of 0.16, which corre-

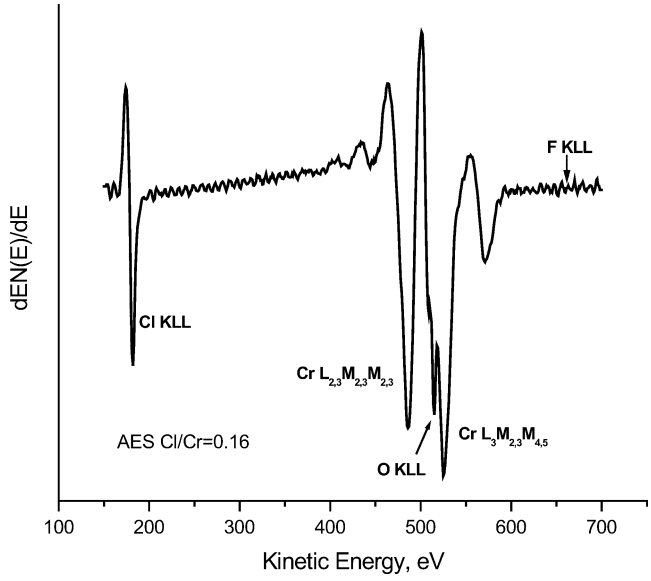

Fig. 5. AES spectrum of a surface deactivated by the reaction of $CFCl{=}CH_2$ to HC≡CH. A Cl/Cr ratio of 0.16 is found for the surface deactivated by deposited halogen atoms. Deposited F is not observed because it undergoes rapid electron-stimulated removal from the surface. See text for discussion.

sponds to a surface deactivated by $CFCl{=}CH_2$ under TDS conditions.

The reaction stoichiometry for forming $HC{\equiv}CH$ from $CFCl{=}CH_2$ decomposition requires that chlorine and fluorine be removed from the reactant molecule in equal proportions. Therefore, assuming that all of the removed halogen remains on the surface, a surface that has been halogenated by $CFCl{=}CH_2$ decomposition to form $HC{\equiv}CH$ is expected to accumulate equal amounts of chlorine and fluorine, regardless of the level of halogenation. As indicated above, a surface with a 1:1 $Cl_{(s)}$:Cr^{3+} ratio has an AES Cl/Cr ratio of 0.32. The AES Cl/Cr of 0.16 measured for surfaces deactivated by $CFCl{=}CH_2$ TDS suggests that half of the cation sites are covered by chlorine and half by fluorine. However, the fluorine cannot be seen using AES due to electron-stimulated loss from the surface. Deactivation of the surface is attributed to site blocking by $F_{(s)}$ and $Cl_{(s)}$, but only chlorine may be seen using electron-stimulated AES. Nearly 100% of the cations at the deactivated surface are expected to be capped by halogen adatoms.

The integrated TDS data shown in Fig. 4 demonstrate an increase in $CFCl{=}CH_2$ uptake and a coincident increase in $HC{\equiv}CH$ product for low total exposures. The increase and subsequent decrease in total desorption quantities shown in Fig. 4 demonstrates that the $CFCl{=}CH_2$ sticking coefficient is a function of the degree of surface halogenation. The 20-K increase in the $CFCl{=}CH_2$ desorption temperature suggests that the strength of the $CFCl{=}CH_2$/surface interaction is also a function of the degree of surface halogenation. For halogen coverage of up to approximately one-third of surface cations (Cl/Cr=0.055, and assuming an equivalent amount of surface F), the $CFCl{=}CH_2$ sticking coefficient increases. For higher coverages of surface halogen, the sticking coefficient declines, reaching approximately 20% of the maximum value by 1.0 L of total $CFCl{=}CH_2$ exposure for a series of 0.13-L doses. The observed increase in the amount of acetylene made for low total exposures is attributed to an increase in the $CFCl{=}CH_2$ sticking coefficient.

4.3. $CFCl{=}CH_2$ thermal desorption from an oxygenated surface

$CFCl{=}CH_2$ TDS over surfaces that were preexposed to oxygen showed that the surface reaction is completely inhibited over an oxygen-terminated surface. TDS experiments using successive 0.03 L doses of $CFCl{=}CH_2$ over the oxygen-saturated surface yielded no $HC{\equiv}CH$ or any other gas-phase product. Specifically, no H_2, H_2O, CO, or CO_2, nor any carbon-, fluorine-, or chlorine-containing compounds (other than $CFCl{=}CH_2$) were observed during TDS experiments. Additionally, AES of the oxygenated surface following thermal desorption showed no indication of surface chlorine or carbon. The TDS and AES data clearly demonstrate $CFCl{=}CH_2$ decomposition does not occur over an oxygen-saturated surface.

5. Discussion

The 1,1-dihaloelimination (decomposition) reaction of $CFCl{=}CH_2$ to acetylene over Cr_2O_3 $(10\bar{1}2)$ was found to occur readily over a nearly stoichiometric (1×1) surface. The overall reaction may be represented as

$$ClFC{=}CH_2 \rightarrow HC{\equiv}CH_{(g)} + Cl_{(s)} + F_{(s)}.$$

The deposition of halogen ($Cl_{(s)}$ and $F_{(s)}$) on the surface is coincident with changes in surface reactivity and the eventual deactivation of the surface towards the decomposition reaction. The occurrence of a 1-chloro, 1-fluoro elimination reaction is somewhat unexpected because of its lack of precedent in the catalysis literature. To our knowledge, this is the first documentation of a dihaloelimination reaction for gas phase haloethenes over Cr_2O_3 under any conditions.

5.1. Low-temperature (350-K) acetylene product

The occurrence of two features for the acetylene product in $CFCl{=}CH_2$ thermal desorption spectra indicate that two energetically different desorption processes occur. Comparison of dosed acetylene and product acetylene desorption traces demonstrates that the low-temperature peak is desorption-limited and the high-temperature peak is reaction-limited. This suggests that the 350 K portion of the product acetylene signal is the result of $CFCl{=}CH_2$ that reacts to form acetylene at a lower temperature and then remains adsorbed on the surface until the acetylene desorption temperature is reached. Acetylene formation may occur upon adsorption at 170 K, or at any intermediate temperature during a TDS run, up to 350 K. The rate limiting step for $HC{\equiv}CH$ desorption via the low-temperature reaction channel is attributed to the desorption of a molecular surface species. Assuming a preexponential of 10^{13} s^{-1} an apparent first-order activation energy for desorption of 90 kJ/mol is found for the desorption limited acetylene peak [12].

During $CFCl{=}CH_2$ TDS, the peak desorption temperature for the low-temperature $HC{\equiv}CH$ product peak undergoes a significant shift to lower temperature (see Fig. 2). The majority of this temperature shift occurs for total $CFCl{=}CH_2$ exposures of 0.40 L and less (Fig. 2). The surface AES Cl/Cr ratio also changes rapidly throughout this range of $CFCl{=}CH_2$ exposure. The range of AES Cl/Cr ratios (0.0–0.08) for a series of 0.13-L doses up to a total exposure of $\sim$ 0.4 L of $CFCl{=}CH_2$ in TDS corresponds to a range of surface halogen coverage of approximately zero to 50% coverage of surface Cr^{3+} cations. Therefore, the shift in the low-temperature acetylene feature from 350 to 270 K is attributed to a decrease in the activation energy of desorption caused by the modification of the surface by F(s) and Cl(s).

The additional $HC{\equiv}CH$ produced during initial $CFCl{=}CH_2$ TDS runs is adsorbed almost entirely into the low-temperature state. Fig. 4 shows that the maximum amount of acetylene is produced over a surface having a total

$CFCl{=}CH_2$ exposure of around 0.25 L and a Cl/Cr ratio of 0.055. This level of surface chlorination corresponds to approximately one-third of surface cations being covered by a 1:1 mixture of $F_{(s)}$ and $Cl_{(s)}$. Comparison of the total integrated desorption area for reactant and product shows that the increase in desorption quantities are attributable to an increase in the sticking coefficient for $CFCl{=}CH_2$ over the Cr_2O_3 $(10\bar{1}2)$ surface. The increase in product HC≡CH demonstrates that the surface is "activated" toward $CFCl{=}CH_2$ decomposition due to an increase in the $CFCl{=}CH_2$ sticking coefficient. The total of desorbing species shows a sharp decline as more than one-third of surface cations become halogenated. The decline in products observed as the surface halogenation increases is attributed to cation site blocking by adsorbed halogen.

There are no previous reports in the literature of acetylene or $CFCl{=}CH_2$ adsorption over Cr_2O_3 single crystals in UHV, but both molecular and dissociative HC≡CH adsorption has been reported over single-crystal metal and metal oxide surfaces [21,22]. Vohs and Barteau [23] report that HC≡CH is adsorbed over ZnO $(000\bar{1})$ in both molecular and dissociated forms. The molecularly bound state is reported to desorb at around 200 K. Dissociative adsorption results in the formation of a surface acetylide (HC≡C–) that is stable until decomposition to CO, CO_2, and water at 780 K. The thermal stability of this acetylide is much higher than observed for the 270–350 K desorption-limited acetylene feature. The lower thermal stability, the absence of surface carbon in AES experiments, and the lack of CO, CO_2, and water in thermal desorption indicate that the adsorbed species is not an acetylide and suggests a simple molecular acetylene adsorbate.

5.2. High-temperature (470-K) acetylene product

The absence of a 470-K feature in the TDS spectra of dosed acetylene demonstrates that this high-temperature channel is reaction-limited. As the intensity of the 470-K feature declines during surface deactivation, no significant change in peak desorption temperature is observed. The constant peak temperature is characteristic of first-order desorption kinetics. The first-order activation energy for desorption from this state is about 125 kJ/mole [12] assuming a normal first-order preexponential of 10^{13} s^{-1}.

The surface intermediate associated with the reaction-limited production of acetylene cannot be identified definitively with only TDS and AES data. However, the molecular properties of $CFCl{=}CH_2$, along with precedents from the organometallic literature [24,25,29,30,32] can provide some insight into possible reaction pathways, surface intermediates, and rate limiting steps. Table 1 shows the bond dissociation energies for $CFCl{=}CH_2$, predicted from CBS-Q calculations with Gaussian 94 [26]. The weakest bond in $CFCl{=}CH_2$ is the C–Cl bond, regardless of whether homolytic or heterolytic bond breaking is considered. Also, it has been demonstrated using AES that the decomposition of $CFCl{=}CH_2$ deposits chlorine on the sample. It is, therefore, reasonable to assume that the initial reaction step is the dissociative adsorption of $CFCl{=}CH_2$ via carbon–chlorine bond cleavage. In addition to the lower C–Cl bond dissociation energy predicted for homolytic cleavage (Table 1), a homolytic bond breaking process is also expected by analogy to the studies of Gellman and co-workers [27,28]. They report homolytic carbon–chlorine bond cleavage for the adsorption of several dichloroethane compounds over Pd (111). Cleavage of the C–Cl bond upon dissociative adsorption is expected to result in the formation of a surface fluorovinyl species and adsorbed chlorine.

Table 1
Predicted bond dissociation energies for $CFCl{=}CH_2$

Products	Bond dissociation energies[a]
$CH_2{=}CF + Cl$	403 kJ/mol
$CH_2{=}CCl + F$	507 kJ/mol
$CFCl{=}CH + H$	480 kJ/mol
$CH_2{=}CF^+ + Cl^-$	900 kJ/mol
$CH_2{=}CCl^+ + F^-$	965 kJ/mol

[a] CBS-Q energies from Gaussian 94 [26].

Following dissociative adsorption, the reaction is postulated to proceed via α-fluorine elimination to a vinylidene surface intermediate and adsorbed fluorine. The Group (VI) transition metals chromium, molybdenum, and tungsten are known to form vinylidene complexes [29], and α-elimination of halogen from 1-haloolefins is a well-known method of preparing these organometallic complexes [30,31]. Carbenes have also been suggested as intermediates in hydrodehalogenation reactions of haloalkanes [32–34], the reaction of $CH_3CCl_2CH_3$ on Cu (100) [35], and for adsorption of 1,1-dichloroethane [36] over palladium catalysts. Chlorovinylidene has also been suggested as one of a number of possible surface intermediates in the decomposition of TCE over PdCu (110) [37]. The final reaction step to acetylene over Cr_2O_3 $(10\bar{1}2)$ requires the isomerization of vinylidene to acetylene via a 2,1 hydrogen shift.

The acetylene product in both the desorption-limited and reaction-limited states is thought to be produced via the same overall surface mechanism, though the rate-limiting steps are different. For the low-temperature reaction channel, the desorption of molecular acetylene is the rate-limiting step; hence the hydrogen rearrangement must occur on the surface. In the high-temperature channel, whether the surface vinylidene desorbs as a carbene ($H_2C{=}C$:) and isomerizes to HC≡CH in the gas phase, or a 2,1-hydrogen shift occurs on the surface is uncertain. The proposed overall mechanism for $CFCl{=}CH_2$ decomposition is represented in Scheme 1.

The rate-limiting step for the 470-K reaction channel must be a step prior to the formation of molecular acetylene, which would be expected to desorb at around 350 K. In the pathway described in Scheme 1, both α-elimination and hydrogen rearrangement (vinylidene isomerization) are possible rate-limiting steps for the high-temperature channel. If

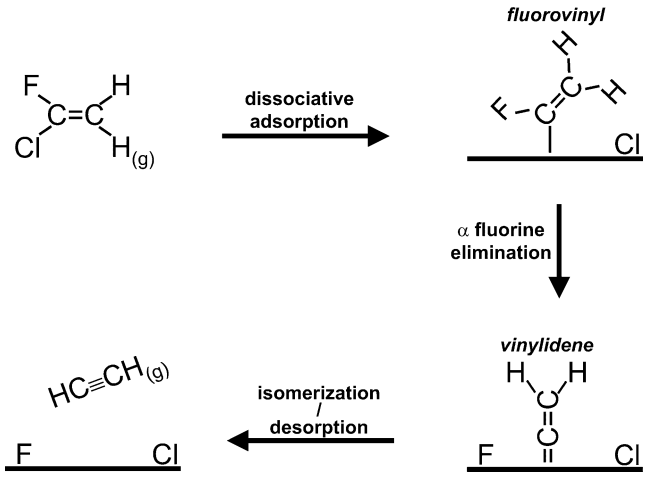

Scheme 1. Proposed reaction sequence involving fluorovinyl and vinylidene surface intermediates. The initial dehalogenation step is Cl elimination during dissociative adsorption, with the final removal of F by α elimination from the fluorovinyl to form surface vinylidene.

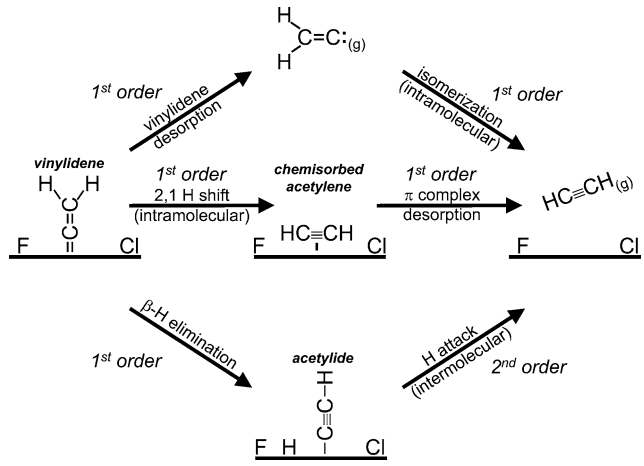

Scheme 2. Possible routes from vinylidene to gas-phase acetylene. The top route represents the desorption and gas-phase isomerization of vinylidene, while the middle and bottom routes represent possible surface routes to acetylene. The three initial first-order reactions from vinylidene are possible rate limiting steps for the high-temperature acetylene production channel.

the loss of fluorine from the α-carbon of the adsorbed fluorovinyl is rate-limiting, then the process will have first-order desorption kinetics, as seen in the 470-K acetylene peak. If the rearrangement/desorption process is rate-limiting, the kinetics are expected to depend on the details of the elementary steps involved. The rearrangement/desorption step might occur by three pathways to form gas-phase acetylene, each pathway containing possible first order rate-limiting steps, as shown in Scheme 2.

From the proposed vinylidene intermediate, a hydrogen rearrangement (vinylidene isomerization) must occur to form the acetylene molecule (HC≡CH). Gas-phase isomerization and surface rearrangement mechanisms may be envisioned to achieve the hydrogen shift. While the observation of a desorption-limited acetylene peak at 350 K implies that hydrogen rearrangement can occur on the surface, the possibility of gas-phase rearrangement at 470 K cannot be disregarded. First order desorption kinetics are expected for vinylidene desorption and gas-phase isomerization to acetylene. Vinylidene desorption followed by gas-phase isomerization is represented in the top pathway in Scheme 2.

Assuming rearrangement of the vinylidene occurs on the surface at 470 K, two possibilities can be considered: (1) β-hydride elimination (acetylide formation) followed by hydrogen addition to the α-carbon to form HC≡CH, and (2) an intramolecular 2,1-hydrogen shift to form HC≡CH, which desorbs immediately. The two possible surface rearrangements are represented as lower and middle pathways, respectively, in Scheme 2. Each possible pathway is addressed below.

An intermolecular rearrangement to acetylene via surface acetylide (1) is shown in the lower pathway in Scheme 2. TDS data indicates that the rate-limiting step is first order. Therefore, since the reaction of acetylide with surface hydrogen should be a second order process, β-hydride elimination would be rate-limiting if the isomerization were intermolecular. Vohs and Barteau [25] report the formation of an acetylide species following acetylene adsorption at 160 K on ZnO (0001). However, the acetylide intermediate on ZnO reacts at 780 K, a temperature significantly higher than observed in the present case, to form CO, CO_2, and H_2O. Additionally, our TDS experiments with $CFCl{=}CH_2$ and preadsorbed D_2 produced no DC≡CH, which would demonstrate that the reaction mechanism proceeds through an acetylide intermediate. However, as mentioned above, the results are not conclusive because D_2 was found to desorb at 285 K, well below the 470-K reaction temperature. Because no decomposition products (CO, CO_2, H_2, or surface carbon) are observed and because no DC≡CH was observed, acetylide formation (i.e., intermolecular rearrangement) is considered less likely than intramolecular rearrangement.

The reverse of the intramolecular hydrogen shift [2] proposed above has been observed to occur on the metals palladium, and platinum via adsorption of acetylene gas and a 1,2 hydrogen shift to form surface vinylidene [38–40]. While vinylidene species have been identified on metal surfaces, they are consistently reported to decompose rather than desorb [38,41–43]. Ormerod et al. [38] report that vinylidene formed from the adsorption of acetylene on Pd (111) decomposes at 480 K, nearly identical to the 470-K peak desorption temperature observed for the high-temperature acetylene feature. If the surface reaction proceeds via an intramolecular rearrangement, as shown in the middle pathway, then the rate-limiting step could be either intramolecular rearrangement of vinylidene to acetylene or the initial α-fluorine elimination from a surface fluorovinyl intermediate to produce vinylidene.

Based upon the preceding discussion, an intramolecular 2,1 hydrogen shift in surface vinylidene to form acetylene is considered the most likely pathway for the hydrogen rearrangement. A limited capacity for backbonding by chromium cations on the stoichiometric Cr_2O_3 $(10\bar{1}2)$ sur-

face has been indicated by TDS experiments using dosed CO. The low activation energy for desorption (50 kJ/mol) for the well-known electron acceptor CO indicates that the surface–adsorbate interaction is predominantly sigma and that backbonding is minimal on the stoichiometric surface. The literature [22,44] clearly demonstrates that electron density donated to an adsorbed vinylidene through backbonding with metal centers tends to weaken the C=C bond, as evidenced by an increase in the C=C bond distance. It is suggested that the lack of backbonding from Cr^{3+} cations on Cr_2O_3 ($10\bar{1}2$) may favor the rearrangement/desorption of an adsorbed vinylidene over the complete decomposition that is observed on metal surfaces.

5.3. $CFCl{=}CH_2$ desorption

The low peak desorption temperature (180–200 K) for $CFCl{=}CH_2$ suggests that this desorption feature is associated with a molecular surface species. Freund and co-workers [10,11] have studied the adsorption of ethene in UHV on Cr_2O_3 (0001) films. Following doses of 0.1 L they reported an ethene peak desorption temperature of 220 K. Freund and co-workers used RAIRS, EELS, and XPS to argue that molecular ethene is bound via a π-complex to stoichiometric Cr_2O_3 (0001) films at five-coordinate Cr^{3+} sites. Based upon the similarity in desorption temperatures, it is suggested that $CFCl{=}CH_2$ forms a similar molecular surface species at cation sites on Cr_2O_3 ($10\bar{1}2$). The first-order activation energy for desorption for this adsorbate is approximately 46 kJ/mol, as calculated by the Redhead method [12] assuming a normal first-order preexponential of 10^{13} s^{-1}.

Following initial doses of 0.03 L over a (1×1) stoichiometric surface, molecular $CFCl{=}CH_2$ is observed to desorb at around 180 K. Following a total exposure of 0.10 L the $CFCl{=}CH_2$ peak desorption temperature shifts to 200 K while the amounts of both reactant and acetylene product are observed to increase. It is apparent that the increase in the amount of $CFCl{=}CH_2$ desorption is the result of an increased sticking coefficient. The 20-K upward shift in $CFCl{=}CH_2$ peak desorption temperature indicates an increase in the ΔH_{ads}. Both of these effects are attributed to the deposition of a favorable amount of halogen (approximately one-third cation coverage) on the sample surface.

Interestingly, Freund and co-workers found that submonolayer coverages of sodium on Cr_2O_3 (0001) films can strengthen of the chromium/ethene interaction "slightly." They suggested that charge redistribution at the surface caused by the presence of sodium induces a change in the ethene bonding mode from the π-complex suggested over a stoichiometric surface to a di-σ complex at a single surface cation [10]. The stronger binding in the presence of sodium was attributed to a through-surface effect because it was found that sodium coverage of a monolayer or more would block all ethene adsorption, except at defects.

Several comparisons may be drawn between the work of Freund and co-workers [10,11] and the effect of halogen deposition upon $CFCl{=}CH_2$ desorption. The molecularly adsorbed states of ethene and $CFCl{=}CH_2$ at Cr^{3+} sites are proposed to be similar π-complexes having approximately the same molecular orientation and surface bond strength over a stoichiometric surface. In addition, when approximately one-third of surface Cr^{3+} cation sites are capped by adsorbed halogen, a slight stabilization of $CFCl{=}CH_2$ at neighboring Cr^{3+} cation sites occurs. TDS experiments demonstrate this stabilizing effect by the increase (20 K) in the peak desorption temperature for $CFCl{=}CH_2$ and the observed increase in the $CFCl{=}CH_2$ sticking coefficient. It is suggested that this effect is due to the redistribution of charge at the Cr_2O_3 ($10\bar{1}2$) surface caused by halogen deposition, as proposed by Freund and co-workers [10] for the adsorption of sodium over the (0001) surface. The difference in ionic charges expected for sodium and chlorine adatoms make their similar effect upon the surface–adsorbate interaction surprising. The nature of this through-surface effect is not understood.

After TDS experiments reach about 1.0 L of total $CFCl{=}CH_2$ exposure, the surface is completely deactivated and the $CFCl{=}CH_2$ molecular feature at 180 K no longer contains any significant contribution from the 200-K shoulder observed for lower total exposures. AES experiments suggest that site blocking by both chlorine and fluorine is responsible for the eventual deactivation of the surface during $CFCl{=}CH_2$ TDS. Site blocking was also reported by Freund and co-workers as the reason for the attenuation of ethene adsorption at monolayer coverages of chlorine and sodium on Cr_2O_3 (0001) [10,11]. The decrease in the amount of adsorbed $CFCl{=}CH_2$ over a halogen-saturated surface relative to the nearly stoichiometric surface is an indication of site blocking by the halogen adatoms.

5.4. Activity of Cr_2O_3 ($10\bar{1}2$)

The amount of product $HC{\equiv}CH$ formed during a TDS series of consecutive $CFCl{=}CH_2$ doses (0.03–0.13 L) is observed to increase initially and then to steadily decline. For the series of 0.06-L $CFCl{=}CH_2$ doses shown in Fig. 2, the production of $HC{\equiv}CH$ is maximized for a total dose of around 0.19 L, and the increase is associated with the desorption-limited acetylene peak. This maximum is associated with an approximate one-third coverage of surface cations by adsorbed halogen. The "activating" effect of surface halogen for $CFCl{=}CH_2$ decomposition can be explained as a through-surface effect that increases the strength of the $Cr^{3+}/CFCl{=}CH_2$ interaction at neighboring cations sites. These results suggests the existence of an optimal surface ensemble consisting of bare Cr^{3+} sites in combination with neighboring halogenated cations in approximately a 2:1 ratio at the surface. Halogenation of the surface beyond the optimal halogen coverage blocks available cations sites and eventually causes surface deactivation.

The necessity of a surface activation period before Cr_2O_3 microcrystalline powders become active for halogen exchange has been well documented in the literature [3,4,45,46].

Activation of the Cr_2O_3 catalyst in these cases has been attributed to the reduction of high-valent chromium species to Cr^{3+} followed by the formation of chromium halides at the surface via oxidation of the HCFC gas. Coulson and co-workers [46] have reported that the reduction of high-valent chromium ions to produce coordinately unsaturated Cr^{3+} centers is the initial step in the catalyst activation process. The lack of activity observed for the oxygen-saturated Cr_2O_3 $(10\bar{1}2)$ surface in this work is in agreement with the suggestion of Coulson and co-workers [46] as it demonstrates that coordinately unsaturated Cr^{3+} centers are also a prerequisite for $CFCl{=}CH_2$ decomposition to acetylene. $CFCl{=}CH_2$ exposures under the thermal desorption conditions of this study are not capable of reducing oxygenated surface cations on the Cr_2O_3 $(10\bar{1}2)$ surface.

Coulson and co-workers [46] have studied the disproportionation of CHF_2Cl over microcrystalline Cr_2O_3 catalyst. They reported that coordinately unsaturated Cr^{3+} cations formed during the initial reduction step were active for the oxidation of CHF_3 and CHF_2Cl to CO, CO_2, HF, and H_2O. They also observed the simultaneous uptake of halogen by the surface during oxidation and suggest that the replacement of surface lattice oxygen by halogen makes the surface active for CHF_3 and CHF_2Cl disproportionation [46]. Kemnitz and co-workers [3] have reported similar results following CF_2Cl and CHF_2Cl exposures over α-Cr_2O_3 powders. No evidence for the replacement of lattice oxygen by chlorine or fluorine was observed over the Cr_2O_3 $(10\bar{1}2)$ surface under the conditions of this study.

Coulson and co-workers [46] also demonstrated that the disproportionation of CHF_2Cl was inhibited over catalysts that were preexposed to the Lewis base dimethyl ether. They found that the uptake of dimethyl ether is directly proportional to the activity of the catalyst for disproportionation, suggesting that an increase in Lewis acidity is coincident with the onset of catalytic activity. They also report that Lewis acidity is greatest for cation sites that had been fluorinated and remained coordinately unsaturated. An increase in site Lewis acidity as a result of surface halogenation is also indicated over the Cr_2O_3 $(10\bar{1}2)$ surface studied in this work by the 20-K increase in $CFCl{=}CH_2$ desorption temperature observed following partial halogenation of a nearly stoichiometric surface. If the $Cr^{3+}/CFCl{=}CH_2$ bonding interaction is predominantly a sigma donation, as described above, then the increase in $CFCl{=}CH_2$ desorption temperature can be attributed to an increase in Lewis acidity at neighboring unhalogenated Cr^{3+} sites. In this work, the increase in active site Lewis acidity is limited to the "through-surface" effect because once halogenated, a Cr^{3+} cation on the Cr_2O_3 $(10\bar{1}2)$ surface is fully coordinated, and is no longer active for $CFCl{=}CH_2$ decomposition into acetylene.

Kemnitz and co-workers [3] studied chlorine/fluorine exchange reactions for various two-carbon HCFC compounds over powdered Cr_2O_3 and attribute the onset of activity to the formation of an active crystalline phase at the surface which resembles β-CrF_3 in structure. They proposed active surface sites for fluorination contain fluorinated Cr^{3+} cations that are coordinately unsaturated and are strong Lewis acids. The halogenated Cr_2O_3 $(10\bar{1}2)$ surface would not be expected to demonstrate activity based upon analogy to the work of Kemnitz and co-workers [3] because the halogenated Cr^{3+} sites are fully coordinated and inaccessible to adsorbing HCFC molecules.

While the reactions involved during the "activation" treatments are ill-defined in the literature, most workers in the area agree that Cr_2O_3 powders are only active toward HCFC fluorine-for-chlorine exchange (fluorination) reactions over fluorinated cation sites [3,6,47]. It seems likely that the reactivity of $CFCl{=}CH_2$ observed over the nearly stoichiometric Cr_2O_3 $(10\bar{1}2)$ surface is due to the presence of five-coordinate Cr^{3+} cations. It is suggested that the decomposition $CFCl{=}CH_2$ and similar HCFC compounds may play a role in the deposition of halogen on the Cr_2O_3 surface during the "activation" of Cr_2O_3 catalysts for halogen exchange reactions [3,4,6,46].

Surface deactivation has also received much attention in the literature in studies of halogen exchange reactions over Cr_2O_3 powders. Deactivation of powdered catalysts has been attributed to carbon deposition [1] and to the formation of inactive crystalline phases at the surface that sterically isolate cations from the surface [3]. In this work, it is apparent from the AES data that deactivation of the Cr_2O_3 $(10\bar{1}2)$ surface toward $CFCl{=}CH_2$ decomposition occurs due to site blocking because nearly 100% of surface cations are coordinated to adsorbed halogen on a deactivated Cr_2O_3 $(10\bar{1}2)$ surface. No carbon was detected on surfaces that were deactivated by $CFCl{=}CH_2$ exposure under any conditions.

6. Conclusions

The 1,1-dihalo-elimination reaction of $CFCl{=}CH_2$ over Cr_2O_3 $(10\bar{1}2)$ has been investigated under UHV conditions. The products are acetylene gas and adsorbed chlorine and fluorine. Thermal desorption experiments reveal two acetylene desorption features. The lower temperature feature is a desorption-limited acetylene peak ($E_a = 92$ kJ/mole), while the formation of a stable fluorovinyl or vinylidene surface intermediate is suggested by the occurrence of a higher temperature ($E_a = 124$ kJ/mole) reaction-limited acetylene desorption peak. The deposition of halogen onto the sample surface by the $CFCl{=}CH_2$ decomposition reaction was found to initially increase the $CFCl{=}CH_2$ sticking coefficient and then lead to deactivation of the surface at near saturation halogen coverage of surface cations due to site blocking.

The Cr_2O_3 $(10\bar{1}2)$ surface was found to cease $CFCl{=}CH_2$ decomposition at a Cl/Cr AES ratio of around 0.16, from $CFCl{=}CH_2$ exposures under TDS conditions. The stoichiometry of the reaction suggests that chlorine and fluorine are deposited at an equal rate during TDS experiments. No evidence was seen for the replacement of surface lattice oxy-

gen by halogen. Surfaces that were preexposed to oxygen were found not to react with $CFCl{=}CH_2$.

Acknowledgments

We thank Dr. Wei Li for performing the Gaussian 94 calculations of bond dissociation energies for $CFCl{=}CH_2$. The authors gratefully acknowledge financial support by the Chemical Sciences, Geosciences and Biosciences Division, Office of Basic Energy Sciences, Office of Science, US Department of Energy through Grant DE-FG02-97ER14751.

References

[1] L.E. Manzer, V.N.M. Rao, Adv. Catal. 39 (1993) 329.
[2] L. Rowley, J. Thomson, G. Webb, J. Winfield, A. McCulloch, Appl. Catal. A 79 (1991) 89.
[3] E. Kemnitz, A. Kohne, I. Grohmann, A. Lippitz, W.E.S. Unger, J. Catal. 159 (1996) 270.
[4] S. Brunet, B. Requieme, E. Colnay, J. Barrault, M. Blanchard, Appl. Catal. B Environ. 5 (1995) 305.
[5] M. Vecchio, G. Gropelli, J.C. Tatlow, J. Fluorine Chem. 4 (1974) 117.
[6] E. Kemnitz, K.U. Niedersen, J. Fluorine Chem. 79 (1996) 111.
[7] M. Blanchard, L. Wendlinger, P. Canesson, Appl. Catal. 59 (1990) 123.
[8] D.M.C. Kavanagh, T.A. Ryan, B. Mile, J. Fluorine Chem. 64 (1993) 167.
[9] K.-U. Niedersen, E. Schreier, E. Kemnitz, J. Catal. 167 (1997) 210.
[10] B. Dillmann, F. Rohr, O. Seiferth, G. Klivenyi, M. Bender, K. Homann, I. Yakovkin, D. Ehrlich, M. Baumer, H. Kuhlenbeck, H. Freund, Faraday Discuss. 105 (1996) 295.
[11] I. Hemmerich, F. Rohr, O. Seiferth, B. Dillmann, H. Freund, Z. Phys. Chem. 202 (1997) 31.
[12] P.A. Redhead, Vacuum 12 (1962) 203. First order activation energies of desorption were estimated assuming a normal preexponential of $10^{13}\ s^{-1}$.
[13] D. Scarano, G. Spotto, S. Bordiga, L. Carnelli, G. Ricchiardi, A. Zecchina, Langmuir 10 (1994) 3094.
[14] S.C. York, M.W. Abee, D.F. Cox, Surf. Sci. 437 (1999) 386.
[15] R.J. Lad, V.E. Henrich, Surf. Sci. 193 (1988) 81.
[16] An ion guage sensitivity of 5.9 was used for $CFCl{=}CH_2$. This value was calculated using a correlation by S. George reported in Ref. [18]. A mass spectrometry sensitivity factor of 1.45 was determined experimentally.
[17] An ion guage sensitivity of 1.7 was used for acetylene. This value was calculated using a correlation by S. George reported in Ref. [18]. A mass spectrometry sensitivity factor of 5.34 was determined experimentally for acetylene.
[18] R.L. Brainard, R.J. Madix, J. Am. Chem. Soc. 11 (1989) 3826.
[19] L.E. Davis, N.C. MacDonald, P.W. Palmberg, G.E. Riach, R.E. Weber, Handbook of Auger Electron Spectroscopy, Perkin–Elmer, Eden Prairie, MN, 1976.
[20] Royal Society of Chemistry, Eight Peak Index of Mass Spectra, 3rd ed., 1983.
[21] V.E. Henrich, P.A. Cox, The Surface Science of Metal Oxides, Cambridge Univ. Press, Cambridge, UK, 1996.
[22] M. Albert, J. Yates, The Surface Scientist's Guide to Organometallic Chemistry, Am. Chem. Society, Washington, DC, 1987.
[23] J.M. Vohs, M.A. Barteau, J. Phys. Chem. 91 (1987) 4766.
[24] W.A. Herman, Adv. Organomet. Chem. 20 (1982) 159.
[25] K. Minachev, Y. Khodakov, V. Nakhshunov, Russ. Chem. Rev. 45 (1976) 142.
[26] M.J. Frisch, G.W. Trucks, H.B. Schlegel, P.M.W. Gill, B.G. Johnson, M.A. Robb, J.R. Cheeseman, T. Keith, G.A. Petersson, J.A. Montgomery, K. Raghavachari, M.A. Al-Laham, V.G. Zakrzewski, J.V. Ortiz, J.B. Foresman, J. Cioslowski, B.B. Stefanov, A. Nanayakkara, M. Challacombe, C.Y. Peng, P.Y. Ayala, W. Chen, M.W. Wong, J.L. Andres, E.S. Replogle, R. Gomperts, R.L. Martin, D.J. Fox, J.S. Binkley, D.J. Defrees, J. Baker, J.P. Stewart, M. Head-Gordon, C. Gonzalez, J.A. Pople, Gaussian 94, Revision C. 2, Gaussian, Inc., Pittsburgh, PA, 1995.
[27] C.W. Chan, A.J. Gellman, Catal. Lett. 53 (1998) 139.
[28] G. Zhou, C. Chan, A.J. Gellman, J. Phys. Chem. B 103 (1999) 1134.
[29] M. Bruce, A. Swincer, Adv. Organomet. Chem. 22 (1983) 59.
[30] J.P. Collman, L.S. Hegedus, J.R. Norton, R.G. Fink, Principles and Applications of Organometallic Chemistry, University Science Books, Mill Valley, CA, 1987.
[31] P. Stang, Chem. Rev. 78 (1978) 383.
[32] E. Boyles, D. Coulson, G. Coulston, M. Diebold, P. Gai, G. Jones, C. Kellner, J. Lerou, L. Manzer, P. Mills, V. Rao, Am. Chem. Soc. Sympos. Chem. Characterization Supported Metal Catal. 38 (1993) 847.
[33] S. Deshmuks, J.L. d'Itri, Catal. Today 40 (1998) 377.
[34] Z. Karpinski, K. Early, J.L. d'Itri, J. Catal. 164 (1996) 378.
[35] M.X. Yang, S. Sarkar, B.E. Bent, Langmuir 13 (1997) 229.
[36] V.Y. Borovkov, F. Lonyi, V.I. Kovalchuk, J.L. d'Itri, J. Phys. Chem. B 104 (2000) 5603.
[37] Y. Jugnet, J.C. Bertolini, L.A.M.M. Barbosa, P. Sautet, Surf. Sci. 505 (2002) 153.
[38] R.M. Ormerod, R.M. Lambert, H. Hoffman, F. Zaera, L.P. Wang, D.W. Bennett, W.T. Tysoe, J. Phys. Chem. 98 (1994) 2134.
[39] L.L. Kesmodel, L.H. Dudois, G.A. Somorjai, J. Chem. Phys. 70 (1979) 2180.
[40] G. Vacek, J. Thomas, B. DeLeeuw, Y. Yamaguchi, H. Schaefer, J. Phys. Chem. 98 (1993) 4766.
[41] G.H. Hatzikos, R.I. Masel, Surf. Sci. 185 (1987) 479.
[42] J.A. Gates, L.L. Kesmodel, Surf. Sci. 124 (1983) 68.
[43] M.M. Hills, J.E. Parmeter, W.H. Weinberg, J. Am. Chem. Soc. 109 (1987) 597.
[44] D. Scarano, G. Spoto, S. Bordiga, G. Ricchiardi, A. Zecchina, J. Electron Spectrosc. Relat. Phenom. 64 (1993) 307.
[45] J. Barrault, S. Brunet, B. Requieme, M. Blanchard, J. Chem. Soc. Chem. Commun. 35 (1993) 374.
[46] D.R. Coulson, P.W.J.G. Wijnen, J.J. Lerou, L.E. Manzer, J. Catal. 140 (1992) 103.
[47] A. Kohne, E. Kemnitz, J. Fluorine Chem. 75 (1995) 103.